1993

Radiative Lifetimes, Branching Ratios, and Absolute Transition Probabilities in Cr II and Zn II

Scott D. Bergeson
scott.bergeson@byu.edu

J. E. Lawler

Original Publication Citation
S. D. Bergeson and J. E. Lawler. Radiative lifetimes, branching rations, and absolute transition probabilities in CR II and Zn II. Astrophys. J. 408 (1), 382-388 (1993).

THE ASTROPHYSICAL JOURNAL, 408:382–388, 1993 May 1

RADIATIVE LIFETIMES, BRANCHING RATIOS, AND ABSOLUTE TRANSITION PROBABILITIES IN Cr II AND Zn II

S. D. BERGESON AND J. E. LAWLER
Department of Physics, University of Wisconsin-Madison, Madison, WI 53706
Received 1992 August 28; accepted 1992 October 28

ABSTRACT

New absolute atomic transition probability measurements are reported for 12 transitions in Cr II and two transitions in Zn II. These transition probabilities are determined by combining branching ratios measured by classical techniques and radiative lifetimes measured by time-resolved laser-induced fluorescence. The measurements are compared with branching fractions, radiative lifetimes, and transition probabilities in the literature. The 206 nm resonance multiplets in Cr II and Zn II are included in this work. These multiplets are very useful in determining the distribution of the elements in the gas versus grain phases in the interstellar medium.

Subject headings: atomic data — ISM: abundances — ultraviolet: interstellar

1. INTRODUCTION

Chromium and zinc in the interstellar medium (ISM) are predominantly once ionized and in the ground level. Accurate absolute transition probabilities (or *f*-values) for transitions in these elements to the ground level are vital for correct interpretation of data from orbiting observatories. Particularly important for evaluation of the ISM are the resonance multiplets at 206 nm in Zn II and Cr II. These transitions are used not only for elemental abundance determination, but also gas versus grain phase evaluation in the ISM. The Goddard High Resolution Spectrograph (GHRS) on the *Hubble Space Telescope* (*HST*) provides an opportunity for much improved astronomical observations at these wavelengths.

Theoretical *f*-values exist for transitions in both Zn II (which is isoelectronic with Cu I) and Cr II. Calculations of *f*-values are difficult and are subject to significant errors, particularly for many-electron atoms (Blackwell et al. 1983). The most reliable and broadly applicable experimental method of determining absolute atomic transition probabilities combines accurately measured branching fractions and radiative lifetimes. Recent works on V I (Whaling et al. 1985), Sc I and Sc II (Lawler & Dakin 1989), and Fe I (O'Brian et al. 1991) demonstrate the power of this approach using semiautomated techniques. In this paper we combine new experimental radiative lifetimes, measured by time-resolved laser-induced fluorescence, and branching fractions, measured by classical techniques, and determine accurate absolute transition probabilities for 14 transitions from the two $3d^{10}(^1S)4p\ ^2P^o$ levels of Zn^+ and the three $3d^4(^5D)4p\ z^6p^o$ levels of Cr^+.

The radiance of a spectral line at frequency ν_{ul} from an optically thin, homogenous length of plasma l is

$$I_{ul} = h\nu_{ul} A_{ul} N_u l/4\pi, \tag{1}$$

where A_{ul} is the Einstein *A*-coefficient (transition probability) corresponding to a transition from an upper level u to a lower level l, h is Planck's constant, and N_u is the volume density of atoms in level u in the plasma. The ratio of transition probabilities for two lines from the same upper level is equal to $[I_{ul'}/(h\nu_{ul'})]/[I_{ul''}/(h\nu_{ul''})]$. In our experiment the relative quantities $I_{ul}/(h\nu_{ul})$, branching ratios, of all significant branches from an upper level are measured; their sum is normalized to the reciprocal of the radiative lifetime: branching fractions (complete sets of branching ratios) are thereby converted directly into absolute transition probabilities. By normalizing the branching fractions with radiative lifetimes, we eliminate any need to determine a plasma temperature or even to produce a plasma in local thermodynamic equilibrium. The absorption oscillator strength, f_{lu}, is related A_{ul} by the relation

$$g_l f_{lu} = \lambda_{ul}^2 g_u A_{ul}/(8\pi^2 r_e c)$$
$$= 1.499 \times 10^{-14}(\text{s nm}^{-2})\lambda_{ul}^2 g_u A_{ul}\ , \tag{2}$$

where λ_{ul} is the wavelength of the transition between the upper and lower levels; g_i is the degeneracy of the level, namely $g_i = 2J_i + 1$; r_e is the classical radius of the electron; and c is the speed of light.

2. LIFETIME EXPERIMENT

A schematic of the experiment is shown in Figure 1. The apparatus is that used by O'Brian et al. (1991). Time-resolved laser-induced fluorescence (LIF) on a slow atomic or ionic beam is recognized as a broadly applicable and accurate method for measuring radiative lifetimes. The atomic/ionic beam source is based on a low-pressure, large-bore hollow cathode discharge. That this source has been successful in producing atomic/ionic beams for over 30 different elements, including refractory metals such as tungsten and niobium as well as nonmetals such as carbon and silicon, demonstrates its versatility. The cathode is lined with the element of interest and a 5–50 mA DC discharge is run in 0.5 torr argon. The number of ions in the discharge is dramatically increased, with minimal heating of the cathode, by superposing on the DC discharge a current pulse of 5 μs duration and up to 20 amps. For the Zn atomic/ionic beam, we use a pure Zn liner in our hollow cathode discharge beam source even though the melting point of Zn is quite low (693 K). The Zn liner is not melted and yet sufficient Zn^+ ions are generated in the beam for our measurements. To generate a Cr atomic/ionic beam, we line the cathode with cleaved strips of pure Cr.

The discharge is sealed from the scattering chamber except for a 1.0 mm hole in the bottom of the cathode which is flared outward at 45° to serve as a nozzle for the atomic/ionic beam. A 10 cm diffusion pump keeps the scattering chamber at a much lower pressure (10^{-4} torr argon) than the discharge,

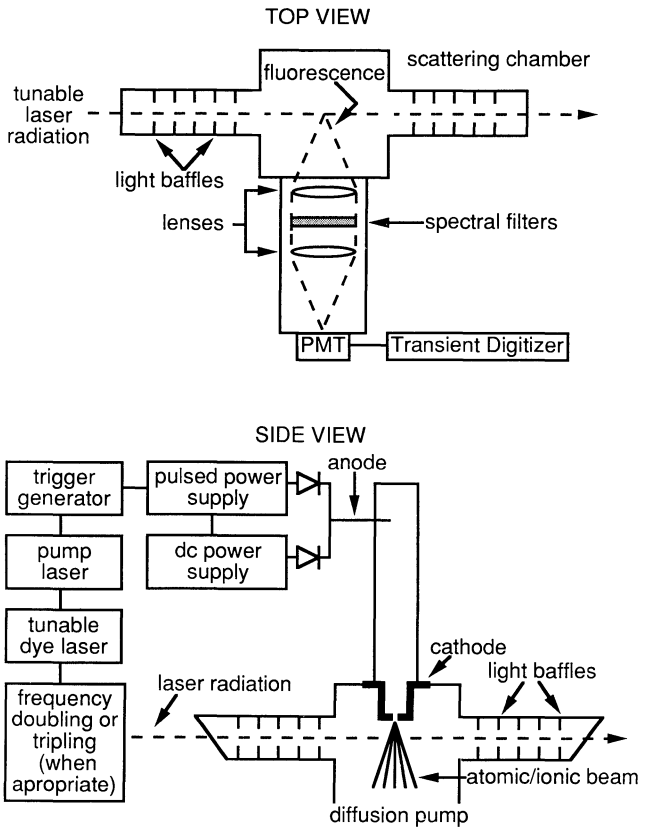

FIG. 1.—Schematic of the radiative lifetime experiment

forming a weakly collimated, optically thin beam which is ideal for laser excitation studies in the scattering chamber. The beam contains neutral and singly ionized species distributed in the ground and virtually all metastable levels. In particular, the metastable $3d^4(^5D)4s\,a^6D$ levels in Cr II, at $\sim$12,300 cm^{-1} above the ground level, are populated sufficiently for laser excitation out of those levels into the three upper Cr II levels included in this study. Neutral species in the beam have kinetic energies slightly above thermal; ions have kinetic energies less than 0.5 eV.

Two different pump lasers are used in this experiment, depending on the wavelength of radiation required. For $\lambda > 205$ nm, we use a N_2 pumped dye laser, designed and built in our lab, which produces a 3 ns duration pulse (FWHM) of 0.2 cm^{-1} bandwidth and up to 40 kW peak power at a 50 Hz repetition rate. A set of beta barium borate (BBO) and potassium dihydrogen phosphate (KDP) frequency doubling crystals extend the lower wavelength limit to 205 nm in the ultraviolet. For $\lambda < 205$ nm, we use a Nd:YAG pumped dye laser, which produces a 10 ns pulse (FWHM) of 0.3 cm^{-1} bandwidth and up to 10 MW peak power at a roughly 27 Hz repetition rate. We frequency triple this radiation in BBO to the edge of the vacuum ultraviolet (VUV). When necessary, VUV radiation is generated via stimulated Raman scattering in liquid nitrogen–cooled hydrogen gas (O'Brian & Lawler 1992).

Tunable pulsed laser radiation crosses orthogonally the atomic beam 1.0 cm below the nozzle. Light baffles are placed along the axis of the laser beam, both inside and outside of the scattering chamber, to reduce scattered laser light. Orthogonal to both the laser and atomic/ionic beams, a photomultiplier tube (PMT) is used to detect the LIF. The N_2 pumped laser system uses an RCA 1P28A PMT; the Nd:YAG pumped laser system uses a Hamamatsu R1220 PMT. For the relatively short lifetimes reported here, two fused silica or MgF_2 lenses comprising an f/1 system focus the intersection of the atomic/ionic and laser beams onto the active region of the photocathode of the PMT. A different fluorescence collection system is used when measuring longer radiative lifetimes to prevent systematic error due to atoms or ions escaping from the detection region before radiating (Marsden et al. 1988).

The signal from the PMT is recorded and averaged using a Tekronix SCD1000 transient waveform digitizer, which has an analog bandwidth of 1 GHz and a sampling rate of up to 200 GHz. The leading edge and first few ns of the signal from the PMT is a convolution of the laser pulse and the LIF. By beginning our analysis of the signal after the laser pulse has ended (about 5 ns after the peak of the fluorescence decay signal), we avoid a deconvolution of the two components. The signal is analyzed using a least-squares fit to a single exponential. Whenever possible, at least two laser wavelengths are used to excite an upper level. This provides confidence that the level is correctly identified and that the lines are not blended. This is not possible for the two $3d^{10}(^1S)4p\,^2P^o$ levels of Zn II for which only one decay branch exists. Reported lifetimes are an average of over 12,000 individual fluorescence decay curves. Statistical uncertainty is less than 0.5% (1 σ) when signals are strong.

The lifetime experiment has a dynamic range from roughly 2 ns to 2 μs. Near the 2 μs end of the range, systematic effects due to atomic motion dominate. An excited atom or ion in the beam can leave the field of view of the light detection apparatus before radiating, artificially shortening the lifetime. This systematic error is completely negligible for the short-lived levels studied here. The finite electrical bandwidth of the detection apparatus is a concern near the 2 ns end of the range. The base of the PMT is wired for very low overall inductance in order to maintain the full electronic bandwidth of the tube. The base includes bypass capacitors in order to provide good linearity to 10 mA of peak anode current and includes small damping resistors to reduce ringing (Harris, Lytle, & McCain 1976). The electrical bandwidth of the detection system has previously been tested by measuring the lifetimes of the $3^1P^o_1$ and $4^1P^o_1$ levels of He I which are known to $\pm$1% from very sophisticated calculations (Salih, Lawler, & Whaling 1985; Wiese, Smith, & Glennon 1966). We also measure the lifetime of the $2s2p\,^1P^o_1$-level of Be I to test the bandwidth of our experiment. We think there is enough evidence to conclude that the radiative lifetime of the $2s2p\,^1P^o_1$ level is 1.85 $\pm$ 0.05 ns. The Sims & Whitten (1973) calculation of the $2s2p\,^1P^o_1$–$2s^2\,^1S_0$ transition probability in Be I approaches the reliability of the best calculations in He I. This and other calculations on Be I are surveyed by Moccia & Spizzo (1985). Accurate ($\pm$1%) experimental lifetimes in the 3 to 4 ns range are available from fast-beam laser measurements on Fe II (Biemont et al. 1991), some of which we also measure to test the electrical bandwidth of our detection apparatus.

Selective laser excitation eliminates repopulation of the upper level through radiative cascade which has troubled beam-foil time of flight measurements. Occasionally in our LIF experiment, a high-lying level of interest decays via infrared transitions to nearby levels which then decay to lower levels producing cascade radiation in the spectrally sensitive region of the PMT (200–700 nm). This radiative cascade through

lower levels is possible in the three upper levels studied in Cr II. The $3d^5\,d^2D$ levels at 47354.44 and 47372.53 cm^{-1} could serve as intermediate even parity levels. However, no evidence for cascade through lower levels is observed in this experiment, probably because selection rules and low frequencies suppress the infrared decay channels. Other systematic errors are avoided by the nature and construction of the experiment. In the beam environment, both radiation trapping and collisional quenching are negligible. This is tested by searching for any change in the observed lifetime while varying the beam intensity and background pressure. The magnetic field in the scattering chamber is kept near zero (<20 mG) when short lifetimes are measured, such as those included in this study. This eliminates the possibility of observing Zeeman quantum beats. The totality of error we conservatively estimate as the greater of $\pm 5\%$ or ± 0.2 ns. This uncertainty cannot easily be identified as a 1 σ or 3 σ uncertainty because photon statistics actually make a negligible contribution to the uncertainty. The uncertainty for these short lifetimes is dominated by the electronic bandwidth, linearity, and overall fidelity of the data acquisition system including the PMT, coaxial cables, and transient digitizer. The previously described "bandwidth tests" of the detection system such as our measurement of short Be I and He I lifetimes are thus very important. Our goal is to have more than 90% of our lifetime measurements accurate to within one uncertainty. We note that the first ion lifetimes measured using this apparatus were in Nb II (Salih & Lawler 1983). These Nb II lifetimes were remeasured by Hannaford et al. (1985) using an experiment of comparable accuracy and precision. The average and root mean squared (rms) difference between Nb II lifetimes measured by Hannaford et al. and lifetimes measured by Salih & Lawler is +0.9% and 3.5%, respectively. All of these lifetimes agreed to within their combined uncertainties.

3. BRANCHING FRACTION EXPERIMENT

Only one electric dipole decay branch exists for the $3d^{10}(^1S)4p\,^2P^o_{1/2}$ and $3d^{10}(^1S)4p\,^2P^o_{3/2}$ levels in Zn II. Thus the transition probability is the reciprocal of the radiative lifetime. The $3d^4(^5D)4p\,z^6P^o$ levels in Cr II have several branches including "allowed" transitions to the $3d^5\,a^6S$ ground level and the $3d^4(^5D)4s\,a^6D$ levels $\sim$12,300 cm^{-1} above the ground level, and intercombination or spin-forbidden transitions to other low-lying even parity levels as well. Figure 2 is a partial Grotrian diagram showing the decay pattern of the $z^6P^o_{5/2}$ level. The decay patterns of the other z^6P^o levels are similar. Comprehensive branching fractions measurements of complex spectra are best made on the powerful 1.0 m Fourier transform spectrometer at the National Solar Observatory at Kitt Peak (O'Brian et al. 1991). However, the measurements for this investigation are few and the spectra are simple, thus we used a simpler apparatus.

The emission source in this experiment is the same hollow cathode discharge used in the lifetime experiment, shown schematically in Figure 3. To avoid possible blends with the Fe I and II spectra in the emission source, the cleaved strips of Cr lining the cathode for the lifetime experiment, which left some of the stainless steel cathode exposed, are replaced by a Cr plated hollow cathode. A slightly wedged fused silica window near the anode transmits the uv light from the discharge, which also serves as the source of the atomic/ionic beam described in the previous section, to an Acton Research Corporation 1.0 m

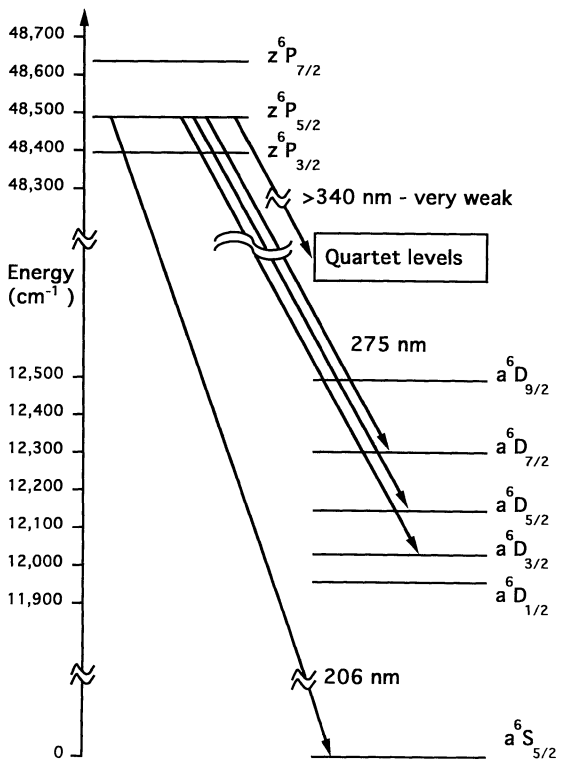

FIG. 2.—Partial Grotian diagram showing the decay of the $z^6P^o_{5/2}$ level of Cr II with approximate vacuum wavelengths. The unspecified quartet levels to which transitions have been observed include the $a^4D_{3/2}$, $a^4D_{5/2}$, $a^4D_{7/2}$, $a^4P_{5/2}$, and $b^4P_{3/2}$ levels (Kiess 1951).

vacuum compatible monochrometer. This Czerny-Turner style monochrometer is equipped with a 2400 lines per mm holographic grating. The reciprocal linear dispersion in the focal plane is nominally 0.41 nm mm^{-1}, the slit widths are adjustable from 5 μm to 3000 μm, and the wavelength scan rate is variable in 9 steps from 0.1 nm per minute to 100 nm per minute. A strip-chart recorder is used to log the signal from a PMT located at the exit slit of the monochrometer. To improve signal to noise in the PMT output, we use an integration circuit with a 0.3 s time constant.

For the emission method we use, no information of plasma parameters, such as the absolute number density of the emitting level or the absolute temperature of the source, is needed. It is also unnecessary for the discharge to be symmetric, homogeneous, or in thermal equilibrium. However, the source must be optically thin and stable over time. When a sample is optically thick, radiation trapping occurs: photons emitted from

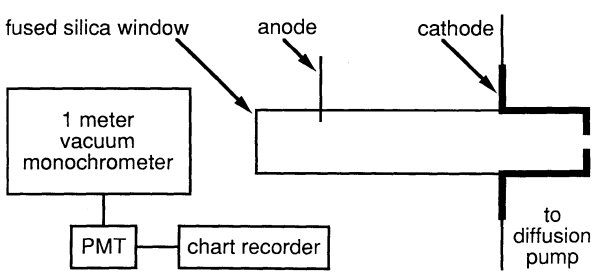

FIG. 3.—Schematic of the branching ratio experiment

one end of the source are reabsorbed by other atoms or ions before they escape the plasma. When lines tied to the ground level are radiation trapped, the other lines from the same upper level appear artificialy strong. We compare branching ratios as a function of DC current, and hence ion density, in the source, and find a low-current region over which the branching ratios remain constant: we are confident the emission source is optically thin. The emission source is largely stable over time, but small slow drifts do occur over the duration of the experiment. We account for this approximately linear drift by alternately measuring lines and averaging the results. The light detection system is linear over two orders of magnitude. Linearity of the detection system is assessed with tested Melles-Griot ultraviolet neutal density filters.

The relative response of the monochrometer-PMT detection system is calibrated as a function of wavelength using an Optronics D_2 lamp. This lamp is a secondary standard of spectral irradiance, not spectral radiance. As such, it has structure in the source and should not be imaged onto the entrance slit. This means that only part of the monochrometer grating and mirrors are illuminated in a calibration run. We compensate for this by varying the position of the D_2 lamp in a plane perpendicular to the optical axis of the system and find no variations in the performance of the monochrometer. Uncertainties in the branching fractions are almost entirely systematic due to the uncetainty in the D_2 lamp calibration. We cannot describe such uncertainties as 1 σ or 3 σ.

4. RESULTS

4.1. Zn II

Each of the $3d^{10}(^1S)4p\,^2P$ levels in Zn II has only one decay branch. The transition probability is the reciprocal of the radiative lifetime. A comparison of radiative lifetimes for these Zn II levels is made in Table 1. The energy levels are from Martin & Kaufman (1970). The number in parentheses following each entry is the uncertainty in the last digit(s) of the entry. The experimentalists cited in Tables 1 and 2 all made an effort to include potential systematic error in their uncertainties. It is prudent in the absence of other information to assume that the uncertainties in these cited works are 1 σ rather than 3 σ uncertainties. We are not aware of any previous LIF measurements for these two levels in Zn II. The various experimental methods and theoretical approaches employed are also noted in the table. Some authors quote only multiplet values and these results are presented on an intermediate line in the table.

4.2. Cr II

Table 2 lists radiative lifetimes for the three $3d^4(^5D)4p\,z^6P^o$ levels including our measurements and those found in the literature. The energy levels in Tables 2 and 3 are from Sugar & Corliss (1985). Vacuum wavelengths calculated from the energy levels are used throughout this work. We note that Martin & Kaufman (1970) published a line list for Zn II and Kiess (1951) published a line list for Cr II. A recent LIF mea-

TABLE 1A

EXPERIMENTAL RADIATIVE LIFETIMES (ns) FOR THE $3d^{10}(^1S)4p\,^2P^o$ LEVELS IN Zn II

Upper Level	Energy (cm^{-1})	This Work	HLLMV[a]	CB[b]	MCHLLMJ[c]	BS[d]	AS[e]	APR[f]	RS[g]	SKA[h]
$^2P^o_{3/2}$	49355.04	2.5(2)	2.1(3)	1.9	2.07(20)	3.1(4)	3.0(3)	3.0(3)	2.4(3)	3.2(2)
$^2P^o_{1/2}$	48481.00	2.5(2)	2.1(4)	0.22	...	3.05(40)		...		

[a] Hultberget al. 1981, beam-foil.
[b] Corliss & Bozman 1962, emission measurements.
[c] Martinson et al. 1979, beam foil.
[d] Bauman & Smith 1970, phase shift method.
[e] Andersen & Sorensen 1973, beam-foil.
[f] Andersen et al. 1976, Hanle effect.
[g] Rambow & Schearer 1976, Hanle effect.
[h] Shaw, King, & Adams 1978, electron-photon delayed coincidence.

TABLE 1B

THEORETICAL RADIATIVE LIFETIMES (ns) FOR THE $3d^{10}(^1S)4p\,^2P^o$ LEVELS IN Zn II

Upper Level	Energy (cm^{-1})	F[a]	McG[b]	MB[c]	CD[d]	CT[e]
$^2P^o_{3/2}$	49355.04	2.6	2.2	2.5	2.9	2.4
$^2P^o_{1/2}$	48481.00			2.7	3.2	2.5

[a] Fischer 1977, nonrelativistic multiconfigurational Hartree-Fock.
[b] McGinn 1969, pseudopotential method. The above value is based on McGinn's radial matrix element and calculated energies. If experimental energies are used instead, the lifetime from McGinn's radial matrix element is 1.7 ns.
[c] Migdalek & Bayles 1979, relativistic model potential including core polarization effects.
[d] Chichkov & Shevelko 1981, one electron approximation including core polarization effects.
[e] Curtis & Theodosiou 1989, model potential including core polarization effects.

TABLE 2

RADIATIVE LIFETIMES FOR THE $3d^4(^5D)4p\,z^6P^o$ LEVELS IN Cr II

UPPER LEVEL	LEVEL ENERGY (cm^{-1})	LASER IN VACUUM (nm)	EXPERIMENT (ns)					THEORY (ns)		
			This Work	SMH[a]	PLC[b]	EGCM[c]	CB[d]	SMH[a]	AL[e]	KP[f]
$z^6P^o_{7/2}$	48,632.12	205.625 276.734	2.4(2)	2.5(1)		3.3(4)	5.7	2.2	2.2	2.0
$z^6P^o_{5/2}$	48,491.10	206.223 276.341	2.4(2)	2.5(1)	3.3(2)	3.3(6) 3.2(4)	3.9	2.2	2.2	2.1
$z^6P^o_{3/2}$	48,398.95	206.616 275.853	2.4(2)	2.4(1)		...	3.5	2.2	2.3	2.1

[a] Schade et al. 1990. Experiment: LIF. Theory: Coulomb approximation with LS coupling assumed.
[b] Pinnington et al. 1973: beam foil.
[c] Engman et al. 1975: beam foil.
[d] Corliss & Bozman 1962: emission measurements, after applying a multiplicative correction of 0.178 to the transition probabilities as suggested by Warner 1967.
[e] Aashamar & Luke 1990: multiconfiguration optimized potential method.
[f] Kurucz & Peytremann 1975: semiempirical calculations.

surement by Schade, Mundt, & Helbig (1990) agrees very well with ours, as is typical among LIF lifetime experiments. Pinnington, Lutz, & Carriveau (1973) measured 3.3 ± 0.2 ns for the multiplet lifetime. Engman et al. (1975) found two very slightly different results for the $z^6P^o_{5/2}$ level based on which particular decay branch they examined. Both Pinnington et al. (1973) and Engman et al. (1975) used the beam-foil technique which has often yielded erroneously long lifetimes due to cascade repopulation. Corliss & Bozman (1962) values after applying a multiplicative correction of 0.178 to the transition probabilities are listed in the tables. This correction was suggested by Warner (1967).

Table 3 is a listing of branching fractions and absolute transition probabilities for transitions from the three Cr II levels. Uncertainties in our absolute transition probabilities for allowed transitions are calculated by combining lifetime and branching fraction uncertainties in quadrature. They are typically $\pm 10\%$ or less. The experimental branching ratios of Allen & Hesthal (1935) and the theoretical branching ratios based on LS coupling for z^6P^o–a^6D multiplet are normalized to agree with our data for transitions among highest J levels, i.e.: $z^6P^o_{7/2}$–$a^6D_{9/2}$, $z^6P^o_{5/2}$–$a^6D_{7/2}$, and $z^6P^o_{3/2}$–$a^6D_{5/2}$. Allen & Hesthal noted in their spectra that the transitions $\lambda_{vac} =$ 276.341 nm, $\lambda_{vac} = 274.445$ nm, and $\lambda_{vac} = 274.284$ nm had superposed ghosts or overlapping lines.

The z^6P^o–a^6D multiplet is definitely not a pure LS multiplet. We make this claim because our measurements of the relative strengths of lines from a common upper level within this multiplet are actually more accurate than indicated by the uncertainties on the branching fractions. The uncertainty on a

TABLE 3

BRANCHING FRACTIONS AND ABSOLUTE TRANSITION PROBABILITIES FOR LINES FROM THE $3d^4(^5D)4p\,z^6P^o$ LEVELS IN Cr II

UPPER LEVEL	LOWER LEVEL	λ IN VACUUM (nm)	BRANCHING FRACTIONS (%)			TRANSITION PROBABILITIES ($10^8\ s^{-1}$)				
			This Work	AH[a]	LS[b]	This Work	CB[c]	AL[d]	KP[e]	BD[f]
$z^6P^o_{7/2}$	$a^6S_{5/2}$	205.625	29.9(14)	...	...	1.25(12)	0.20	1.69	1.97	...
	$a^6D_{5/2}$	274.091	2.18(7)	2.64	2.57	0.091(8)	0.098	0.102	0.077	0.086
	$a^6D_{7/2}$	275.268	13.7(4)	16.4	15.4	0.57(5)	0.40	0.61	0.54	0.51
	$a^6D_{9/2}$	276.735	53.9(11)	53.9	53.9	2.25(19)	1.1	2.15	2.33	1.77
	IC[g]	...	0.2(1)	...	...	0.008(4)	...	...	0.002	...
$z^6P^o_{5/2}$	$a^6S_{5/2}$	206.223	29.3(14)	...	...	1.22(12)	0.22	1.64	1.89	...
	$a^6D_{3/2}$	274.284	7.4(3)	9.9	9.10	0.31(3)	0.17	0.31	0.26	0.29
	$a^6D_{5/2}$	275.154	23.4(7)	25.2	27.7	0.98(9)	0.71	1.01	0.95	0.88
	$a^6D_{7/2}$	276.341	39.0(8)	39.0	39.0	1.63(14)	1.4	1.51	1.71	1.21
	IC	...	1.0(5)	...	...	0.04(2)	0.10	...	0.036	...
$z^6P^o_{3/2}$	$a^6S_{5/2}$	206.616	28.8(13)	...	...	1.20(11)	0.21	1.61	1.87	...
	$a^6D_{1/2}$	274.445	18.1(4)	17.5	24.8	0.75(6)	0.67	0.77	0.72	0.73
	$a^6D_{3/2}$	274.979	27.9(6)	28.3	34.7	1.16(10)	0.89	1.17	1.18	1.01
	$a^6D_{5/2}$	275.853	23.1(5)	23.1	23.1	0.96(8)	0.93	0.88	1.03	0.68
	IC	...	2 (1)	...	...	0.08(4)	0.15	...	0.048	...

[a] Allen & Hesthal 1935, normalized to our data. Experiment: photographic photometry.
[b] Predictions based on LS coupling, normalized to our data. Theory.
[c] Corliss & Bozman 1962. Experiment: emission measurements, after applying a multiplicative correction of 0.178 to the transition probabilities as suggested by Warner 1967.
[d] Aashamar & Luke 1990. Theory: multiconfiguration optimized potential method.
[e] Kurucz & Peytremann 1975. Theory: semi-empirical calculations.
[f] Bates & Damgaard 1949 as calculated by Warner 1967. Theory: Coulomb approximation.
[g] IC stands for intercombination lines.

branching fraction reflects the calibration uncertainty of widely separated lines.

Kiess (1951) observed a total of 12 intercombination lines from these three Cr II levels. We measure the strongest unblended transitions and give an upper limit for all of the intercombination branches out of each level in Table 3. Additional values for these intercombination lines are found in Warner (1967) and Musielok & Wujek (1979).

Aashamar & Luke (1990) have published what is regarded as the most accurate calculations of f-values for dipole allowed transitions in Cr II. Their paper lists both length and velocity calculations for f-values made in two different wave function basis sets. The length values of the oscillator strengths from the transformed nine configuration calculation are converted to transition probabilities for comparison in Tables 2 and 3. The relative transition probabilities of Aashamar & Luke for the z^6P^o–a^6D transitions compare well with our values. The average and rms differences for only the z^6P^o–a^6D transitions is +0.6% and 6.3%, respectively. In their semiempirical calculations, Kurucz & Peytremann (1975) determined log (gf) values for 38 intercombination lines from the three Cr II levels, including those observed by Kiess (1951). Corliss & Bozman (1962) have previously published the only absolute experimental values for all of the allowed branches included in this study. They also measured the transition probabilities for the two strongest intercombination lines: λ_{vac} = 351.283 nm from the $z^6P^o_{5/2}$ level and λ_{vac} = 349.637 nm from the $z^6P^o_{3/2}$ level. The values for intercombination lines from Corliss & Bozman listed in Table 3 represents only these two lines, with the absolute scale reduced. Bates & Damgaard (1949) first outlined the Coulomb approximation for calculating oscillator strengths. Warner (1967) calculates f-values using the method of Bates & Damgaard. We convert these f-values to transition probabilities for inclusion in Table 3. Our final transition probabilities are converted to log (gf) values for the reader's convenience in Tables 4A and 4B.

TABLE 4A

LOG (gf) VALUES FOR TRANSITIONS FROM THE $3d^{10}(^1S)4p\ ^2P^o$ LEVELS IN Zn II

λ IN VACUUM (nm)	LOWER Level	LOWER Energy (cm^{-1})	UPPER Level	UPPER Energy (cm^{-1})	log (gf) ±0.03
202.614	$^2S_{1/2}$	0.00	$^2P^o_{3/2}$	49,355.04	−0.01
206.266	$^2S_{1/2}$	0.00	$^2P^o_{1/2}$	48,481.00	−0.29

TABLE 4B

LOG (gf) VALUES FOR TRANSITIONS FROM THE $3d^4(^5D)4p\ z^6P^o$ LEVELS IN Cr II

λ IN VACUUM (nm)	LOWER Level	LOWER Energy (cm^{-1})	UPPER Level	UPPER Energy (cm^{-1})	log (gf) ±0.04
205.625	$a^6S_{5/2}$	0.00	$z^6P^o_{7/2}$	48,632.12	−0.20
206.223	$a^6S_{5/2}$	0.00	$z^6P^o_{5/2}$	48,491.10	−0.33
206.616	$a^6S_{5/2}$	0.00	$z^6P^o_{3/2}$	48,398.95	−0.51
274.091	$a^6D_{5/2}$	12,147.82	$z^6P^o_{7/2}$	48,632.12	−1.09
274.284	$a^6D_{3/2}$	12,032.58	$z^6P^o_{5/2}$	48,491.10	−0.68
274.445	$a^6D_{1/2}$	11,961.81	$z^6P^o_{3/2}$	48,398.95	−0.47
274.979	$a^6D_{3/2}$	12,032.58	$z^6P^o_{3/2}$	48,398.95	−0.28
275.154	$a^6D_{5/2}$	12,147.82	$z^6P^o_{5/2}$	48,491.10	−0.18
275.268	$a^6D_{7/2}$	12,303.86	$z^6P^o_{7/2}$	48,632.12	−0.29
275.853	$a^6D_{5/2}$	12,147.82	$z^6P^o_{3/2}$	48,398.95	−0.36
276.341	$a^6D_{7/2}$	12,303.86	$z^6P^o_{5/2}$	48,491.10	0.05
276.735	$a^6D_{9/2}$	12,496.44	$z^6P^o_{7/2}$	48,632.12	0.32

5. DISCUSSION

A recent paper by Cardelli et al. (1991) examines the ISM toward the O7.5 IIInf star ξ Persei using the GHRS on the *HST*. Based on theoretical log (gf) values for the 206 nm lines in Cr II that Morton (1991) derived from Aashamar and Luke, it is argued that Cr is depleted from the gas phase. Our newly measured transition probabilities place this argument on a firmer and more quantitative basis. Observations of these lines through the ISM toward other stars using the *International Ultraviolet Explorer* and *Copernicus* already exist (Pwa & Pottasch 1986) and, with our data, the determination of the relative depletion of Cr out of the gas phase may be refined. Similarly, extragalactic measurements of the gas versus grain phase can be made. These resonance and near-resonance transitions in Zn II and Cr II in distant galaxies are redshifted into the optical region when viewed against very distant quasars (Meyer & Roth 1990). High-resolution measurements on these redshifted transitions using ground-based telescopes can be made. In this manner, the time evolution of the gas versus grain phase in the universe can be studied.

This research is supported by the National Aeronautics and Space Administration under grant NAGW-2908. We thank Walter Mrock of U.S. Chrome for chrome plating our stainless steel cathode.

REFERENCES

Aashamar, K., & Luke, T. M. 1990, J. Phys. B, 23, L733
Allen, J. S. V., & Hesthal, C. E. 1935, Phys. Rev., 47, 926
Anderson, T., Poulsen, O., & Ramanujam, P. S. 1976, J. Quant. Spectros. Rad. Transf., 16, 521
Andersen, T., & Sorensen, G. 1973, J. Quant. Spectrosc. Radiat. Transfer 13, 369
Bates, D. T., & Damgaard, A. 1949, Phil. Trans. R. Soc. Lond., A, 242, 101
Biemont, E., Badoux, M., Kurucz, R. L., Ansbacher, W., & Pinnington, E. H. 1991, A&A, 249, 539
Blackwell, D. E., Booth, A. J., Menon, S. L. R., Petford, A. D., & Smith, G. 1983, MNRAS, 204, 141
Bauman, S. R., & Smith, W. H. 1970, J. Opt. Soc. Am., 60, 345
Cardelli, J. A., Savage, B. D., Bruhweiler, F. C., Smith, A. M., Ebbets, D. C., Sembach, K. R., & Sofia, U. J. 1991, ApJ, 377, L57
Chichkov, B. N., & Shevelko, V. P. 1981, Phys. Scripta, 23, 1055
Corliss, C. H., & Bozman, W. R. 1962, Experimental Transition Probabilities for Spectral Lines of Seventy Elements (US NBS Monograph 53)
Curtis, L. J., & Theodosiou, C. E. 1989, Phys. Rev., A39, 605
Engman, B., Guapp, A., Curtis, L. J., & Martinson, I. 1975, Phys. Scripta, 12, 220
Froese Fischer, C. 1977, J. Phys. B, 10, 1241
Hannaford, P., Lowe, R. M., Biemont, E., & Grevesse, N. 1985, A&A, 143, 447
Harris, J. M., Lytle, F. E., & McCain, T. C. 1976, Anal. Chem., 48, 2095
Hultberg, S., Liljeby, L., Lindgard, A., Mannervik, S., & Veje, E. 1981, Phys. Scripta, 22, 623
Kiess, C. C. 1951, J. Res. NBS, 47, 385
Kurucz, R. L., & Peytremann, E. 1975, Smithsonian Astrophys. Obs. Spec. Rep. 362
Lawler, J. E., & Dakin, J. T. 1989, J. Opt. Soc. Am., B6, 1457
Marsden, G. C., Den Hartog, E. A., Lawler, J. E., Dakin, J. T., & Roberts, V. D. 1988, J. Opt. Soc. Am., B5, 606
Martin, W. C., & Kaufman, V. 1970, J. Res. NBS, 74A, 11
Martinson, I., Curtis, L. J., Huldt, S., Litzen, U., Liljeby, L., Masservik, S., & Jelenkovic, B. 1979, Phys. Scripta, 19, 17
McGinn, G. 1969, J. Chem. Phys., 50, 1404
Meyer, D. M., & Roth, K. C. 1990, ApJ, 363, 57
Migdalek, J., & Bayles, W. E. 1979, J. Phys. B, 12, 1113
Moccia, R., & Spizzo, P. 1985, J. Phys. B, 18, 3537
Morton, D. C. 1991, ApJ, 77, 119
Musielok, J., & Wujek, T. 1979, A&AS, 38, 119

O'Brian, T. R., & Lawler, J. E. 1992, A&A, 255, 420
O'Brian, T. R., Wickliffe, M. E., Lawler, J. E., Whaling, W., & Brault, J. W. 1991, J. Opt. Soc. Am., B8, 1185
Pinnington, E. H., Lutz, H. O., & Carriveau, G. W. 1973, Nucl. Instr. Method., 110, 55
Pwa, T. H., & Pottasch, S. R. 1986, A&A, 164, 116
Rambow, F. H. K., & Schearer, L. D. 1976, Phys. Rev. A, 14, 1735
Salih, S., & Lawler, J. E. 1983, Phys. Rev. A, 28, 3653
Salih, S., Lawler, J. E., & Whaling, W. 1985, Phys. Rev. A, 31, 744
Schade, W., Mundt, B., & Helbig, V. 1990, Phys. Rev. A, 42, 1454
Shaw, W. A., King, G. C., & Adams, A. 1978, J. Phys. B, 11, 239
Sims, J. S., & Whitten, R. C. 1973, Phys. Rev. A, 8, 2220
Sugar, J., & Corliss, C. 1985, J. Phys. Chem. Ref. Data, 14, Suppl. 2, 279
Warner, B. 1967, MRAS, 70, 165
Whaling, W., Hannaford, P., Lowe, R. M., Biemont, E., & Grevesse, N. 1985, A&A, 153, 109
Wiese, W. L., Smith, M. W., & Glennon, B. M. 1966, Atomic Transition Probabilities, Vol. I, Hydrogen through Neon (Nat. Stand. Ref. Data Ser. 4, US NBS) (Washington: US Government Printing Office), 11